Euro. Jnl of Applied Mathematics (2017), *vol.* 28, *pp.* 562–575.
doi:10.1017/S0956792516000449

A note on waveless subcritical flow past symmetric bottom topography

R. J. HOLMES and G. C. HOCKING

Mathematics and Statistics, Murdoch University, Perth, Western Australia, Australia
email: rachel.holmes.22@gmail.com, G.Hocking@murdoch.edu.au

(*Received 1 April 2016; revised 30 September 2016; accepted 6 October 2016; first published online 26 October 2016*)

This paper re-examines the problem of the flow of a fluid of finite depth over two Gaussian-shaped obstructions on the stream bed. A weakly nonlinear analysis in the form of the Korteweg–de Vries equation is used to compare with the results of the fully nonlinear problem. The main focus is to find waveless subcritical solutions, and contours showing the obstruction height and separation values that result in waveless solutions are found for different Froude numbers and different obstruction widths.

Key words: Stream flow, free-surface flow, water waves, potential flow

1 Introduction

The problem to be considered is the steady flow of an ideal fluid passing over an obstruction on the base of a stream of finite depth. The fluid is of uniform depth and speed upstream of the obstruction, with a disturbance to the free surface occurring as the fluid hits the obstruction. The main interest in this work is in those solutions for which the fluid returns to uniform flow downstream of the obstruction.

Two Gaussian-shaped obstructions on the stream bed are considered, where waveless solutions occur when waves from the second obstruction cancel the waves from the first obstruction. Cases involving obstructions of both positive and negative heights will be examined. In an earlier paper [12], the authors considered the fully nonlinear problem, and contours in parameter space representing waveless solutions were found. Here, the problem is revisited using a weakly nonlinear analysis in the form of the Korteweg–de Vries (KdV) equation, and comparisons are made with the results of the fully nonlinear problem.

Subcritical solutions with no downstream waves have been calculated by Forbes [8], for the fully nonlinear problem of flow over a semi-elliptical obstruction. Lustri *et al.* [14] considered the flow past submerged bumps and trenches with inclined sides in the asymptotic limit of small Froude number. A number of solutions were computed with trapped waves above the bump or trench and no waves downstream.

Waveless solutions to the weakly nonlinear problem have been found by Dias and Vanden-Broeck [5,7] who, after calculating critical solutions over a single obstruction that had waves upstream, introduced a second obstruction that trapped the waves between the two obstructions. Binder *et al.* [1, 2] used both nonlinear methods and KdV theory to examine the flow over two types of stream bed topography, the first type being two

triangular obstructions on the stream bed and the second type being a single rectangular obstruction. The comment was made that for subcritical flow, the downstream waves could be eliminated by adjusting the obstruction separation in the case of the two triangles, or the length in the case of the rectangular obstruction. In each case, however, the parameter values that result in these waveless solutions were not investigated further.

Shen [16] examined the accuracy of the stationary forced KdV equation for supercritical flow over a bump by comparing with the experimental results of Sivakumaran *et al.* [17] and the computational results of Dias and Vanden-Broeck [4]. It was concluded that the stationary forced KdV equation was a good model for bumps of small to moderate height with a short base.

A popular method, when solving the forced KdV equation for flow over a small bump, is to approximate the obstruction with an appropriate delta function. The shape of the bump can then be essentially neglected as only the area of the bump is required in order to calculate solutions. See, for example, Binder *et al.* [1,2], Dias and Vanden-Broeck [5,7] and Shen [16]. This paper briefly examines the basis of this method by comparing solutions for flow over bumps that have the same area but are of different widths and heights.

This paper follows the work of Forbes [8] and Hocking *et al.* [11], who found solutions to the nonlinear problem of subcritical flow over a semi-elliptical obstruction on the stream bed with no downstream waves, and Holmes *et al.* [12], who found waveless nonlinear solutions for subcritical flow over two Gaussian obstructions. Forbes [8] calculated the ellipse height and length values that would produce waveless solutions at a Froude number of $F = 0.5$, with these results presented as contours in parameter space. Four contours were plotted, with the first two contours merging to form a loop shape at the limiting value of the ellipse height. Hocking *et al.* [11] reproduced and extended these results, showing that subsequent pairs of contours also merged, and this behaviour was shown to occur for a range of Froude numbers from $F = 0.4$ to 0.8.

Holmes *et al.* [12] found the Gaussian obstruction height and separation values that resulted in waveless solutions for a range of Froude numbers from $F = 0.5$ to 0.7. Contours in parameter space representing waveless solutions were found for obstructions of positive and negative heights. Although the contours for obstructions of positive height did not exhibit the merging behaviour as found by Forbes [8] and Hocking *et al.* [11], those for obstructions of negative height did form an interesting pattern in parameter space, with a number of 'zig-zag' and loop shapes observed.

Waveless subcritical solutions are of particular interest and will be the main focus of this paper. As an extension to the work presented by Holmes *et al.* [12], the suitability of the KdV equation for this problem is investigated by computing waveless solutions for flow over two Gaussian obstructions and comparing with the fully nonlinear solutions. Comparisons are made at different values of the Froude number starting with Froude numbers close to $F = 1$, before examining the effect of obstruction width.

2 Problem formulation

The problem to be considered is that of Holmes *et al.* [12], the two-dimensional steady flow of an ideal fluid in a stream of finite depth, disturbed by some bottom topography $\hat{y} = \hat{B}(\hat{x})$. Upstream of the disturbance, the flow has uniform depth and speed. The free surface of the fluid $\hat{y} = \hat{\eta}(\hat{x})$ is initially unknown and computed as part of the solution.

https://doi.org/10.1017/S0956792516000449 Published online by Cambridge University Press

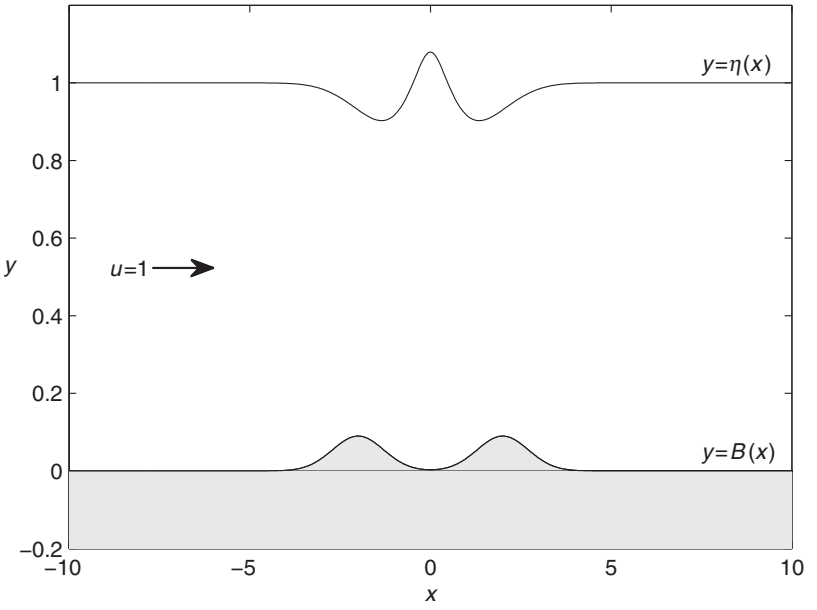

FIGURE 1. Diagram of the non-dimensionalised problem. Upstream of the obstruction, the flow is uniform with unit depth and speed. The obstruction on the stream bed is given by $y = B(x)$ and the unknown free surface by $y = \eta(x)$. The free surface profile and corresponding bottom topography shown here are a solution to the fully nonlinear problem, with obstruction height $\varepsilon = 0.09$, obstruction separation $b \approx 4.002$, obstruction width coefficient $w = 1$ and Froude number $F = 0.6$

The assumption of a steady, two-dimensional flow of an ideal fluid allows a velocity potential ϕ to be defined and requires that Laplace's equation,

$$\nabla^2 \phi = 0, \tag{2.1}$$

be solved subject to boundary conditions on the free surface and the stream bed.

The problem is then non-dimensionalised with respect to the upstream speed c and undisturbed fluid depth h, so that the undisturbed free surface is located at $y = 1$ and the unobstructed stream bed at $y = 0$ with unit speed upstream, as shown in Figure 1. The parameters of the non-dimensionalised problem are then the obstruction size and separation along with the dimensionless flow rate, or Froude number,

$$F = \left(\frac{c^2}{gh}\right)^{\frac{1}{2}}. \tag{2.2}$$

There can be no flow normal to the surface of the fluid and also no flow normal to the stream bed, giving the conditions,

$$\eta'(x) = \frac{v}{u} \quad \text{on} \quad y = \eta(x), \tag{2.3}$$

$$B'(x) = \frac{v}{u} \quad \text{on} \quad y = B(x), \tag{2.4}$$

https://doi.org/10.1017/S0956792516000449 Published online by Cambridge University Press

where u and v are the horizontal and vertical components of the fluid velocity, respectively. We also have the condition of constant pressure on the free surface that gives, from the Bernoulli equation,

$$\frac{1}{2}F^2(u^2+v^2-1)+\eta=1 \quad \text{on} \quad y=\eta(x). \tag{2.5}$$

The bottom topography that we will consider consists of two Gaussian obstructions of height ε and separation b, defined by

$$B(x)=\varepsilon e^{-(w(x-b/2))^2}+\varepsilon e^{-(w(x+b/2))^2}. \tag{2.6}$$

The coefficient w allows us to vary the width of the obstructions, with $w=1$ producing the bottom topography as considered by Holmes *et al.* [12].

3 Nonlinear problem and numerical method

The numerical method used in this paper is as described by Holmes *et al.* [12], where the nonlinear problem was formulated in the physical plane and the resultant nonlinear integral equation was solved numerically using a damped Newton's method. We force the free surface to be symmetric about $x=0$ and allow the obstruction separation value b to be an initial unknown so that it can be computed as part of the solution. The equations are included below, but for a full description of the method, refer to Holmes *et al.* [12].

We define a complex potential $f(z)=\phi+i\psi$, where $\psi(x,y)$ is the stream function, and apply Cauchy's integral formula for any fixed point on the boundary contour, z_0. We take the real part, remove the singularity in the integral and discretise the problem. We obtain an integral equation for the stream bed,

$$\begin{aligned} u_{B_j} = &-\frac{1}{\pi}\int_{-x_L}^{x_L}\frac{(u_B-u_{B_j})(\Delta B-B'\Delta x)+(v_B-v_{B_j})(\Delta x+B'\Delta B)}{\Delta x^2+\Delta B^2}\,dx \\ &+\left[\frac{u_{B_j}}{\pi}\arctan\frac{\Delta B}{\Delta x}\right]_{-x_L}^{x_L}-\left[\frac{v_{B_j}}{2\pi}\log[\Delta x^2+\Delta B^2]\right]_{-x_L}^{x_L} \\ &-\frac{1}{\pi}\int_{x_L}^{-x_L}\frac{u_T((\eta-B_j)-\eta'\Delta x)+v_T(\Delta x+\eta'(\eta-B_j))}{\Delta x^2+(\eta-B_j)^2}\,dx, \end{aligned} \tag{3.1}$$

and an integral equation for the free surface,

$$\begin{aligned} u_{T_j} = &-\frac{1}{\pi}\int_{-x_L}^{x_L}\frac{u_B((B-\eta_j)-B'\Delta x)+v_B(\Delta x+B'(B-\eta_j))}{\Delta x^2+(B-\eta_j)^2}\,dx \\ &-\frac{1}{\pi}\int_{x_L}^{-x_L}\frac{(u_T-u_{T_j})(\Delta\eta-\eta'\Delta x)+(v_T-v_{T_j})(\Delta x+\eta'\Delta\eta)}{\Delta x^2+\Delta\eta^2}\,dx \\ &+\left[\frac{u_{T_j}}{\pi}\arctan\frac{\Delta\eta}{\Delta x}\right]_{x_L}^{-x_L}-\left[\frac{v_{T_j}}{2\pi}\log[\Delta x^2+\Delta\eta^2]\right]_{x_L}^{-x_L}, \end{aligned} \tag{3.2}$$

where $\Delta x=x-x_j$, $\Delta B=B-B_j$ and $\Delta\eta=\eta-\eta_j$.

In order to find the Gaussian separation distances that result in zero waves downstream, we discretise the domain by $x_j=-x_L+(j-1)\frac{2x_L}{2N-1}$, $j=1,2,\ldots,2N$ and specify symmetry,

https://doi.org/10.1017/S0956792516000449 Published online by Cambridge University Press

i.e., $\eta(x) = \eta(-x)$. We make an initial guess for η_j, u_{T_j}, u_{B_j}, $j = 1, 2, \ldots, 2N$, as well as the obstruction separation b, and then fix η_1, hence, we have $3N$ equations in $3N$ unknowns. We find the error in the integral equations (3.1) and (3.2) along with the error in the Bernoulli equation (2.5) and iterate on the first N points using Newton's method to find the free surface elevation $y = \eta(x)$ at $j = 1, 2, \ldots, 2N$, forcing symmetry about $x = 0$ at the beginning of each iteration. The bottom surface $B(x)$ and its derivative $B'(x)$ are specified in advance, whereas the remaining derivatives are approximated using centred finite differences and the integrals approximated using the trapezoidal rule.

The problem was programmed in Fortran and, in general, waveless solutions were graphically reproducible with $N = 400$ points across the free surface from $-x_L$ to x_L with a truncation of $x_L = 20$, as this corresponded to $2N = 800$ points across the full length of the free surface. Increased accuracy could be achieved by decreasing x_L when obtaining solutions for obstructions with shorter separation.

4 Weakly nonlinear problem

This section includes a brief description of the KdV equation for the problem of waveless subcritical flow over topography. The KdV equation is a form of weakly nonlinear analysis and is regularly used in various problems in free surface fluid dynamics. The assumptions made in deriving the KdV equation imply that the results for the problem of flow over topography are valid for Froude numbers close to $F = 1$.

We take the problem as defined in Section 2, but before we non-dimensionalise, we assume that the wavelength L is much greater than the upstream depth h and define a small parameter $\epsilon = \left(\frac{h}{L}\right)^2 \ll 1$. We then non-dimensionalise and expand the velocity potential, free surface and stream bed in powers of ϵ. Full derivations of the KdV equation can be found in several papers, see, for example, [3, 10, 15].

We write the stationary forced KdV equation

$$\frac{1}{6}\eta_{xxx} + \frac{3}{2}\eta\eta_x - (F-1)\eta_x = -\frac{1}{2}B_x, \tag{4.1}$$

and integrate

$$\eta_{xx} + \frac{9}{2}\eta^2 - 6(F-1)\eta = -3B. \tag{4.2}$$

Here, the Froude number is defined as before, $F = \left(\frac{c^2}{gh}\right)^{\frac{1}{2}}$, and $B(x)$ is the bottom topography.

Normally, a phase plane analysis is used when studying the KdV equation in relation to this type of problem. See, for example, Binder *et al.* [1, 2], Pratt [15], Forbes and Hocking [10] and Dias and Vanden-Broeck [5–7]. Often, the obstruction is approximated with an appropriate delta function, meaning that the shape of the obstruction has no effect on the resulting solutions, only the size.

We wish to examine one of the underlying principles of this method by looking at the effect of the obstruction width on the solutions for Froude numbers close to $F = 1$. Consequently, for the purposes of this research, we use an equation solver in MATLAB

https://doi.org/10.1017/S0956792516000449 Published online by Cambridge University Press

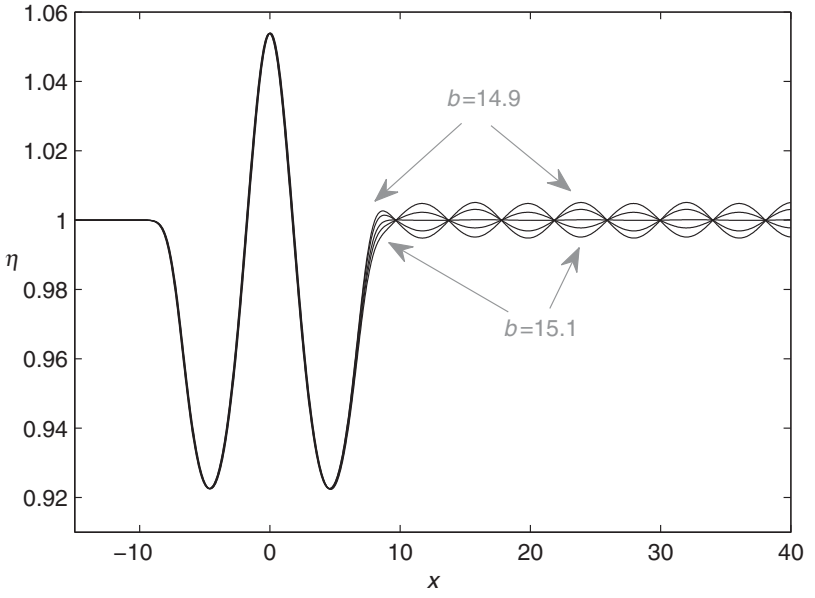

FIGURE 2. Weakly nonlinear free surface profiles for $F = 0.9$ and $\varepsilon = 0.01$ with separations $b = 14.9$, 14.95, 15, 15.05 and 15.1. We observe a change of phase in the waves as b increases, with a waveless solution occurring at $b = 15$.

based on a fourth- and fifth-order Runge–Kutta method to solve the forced KdV equation for a given bottom topography $B(x)$.

5 Results

5.1 A comparison with KdV theory

Contours were plotted showing the obstruction height and separation required for waveless solutions for different width obstructions. This was done for different values of the Froude number, $F = 0.9$, 0.8 and 0.6. The theory used in weakly nonlinear analysis suggests that the size of the obstruction alone can be used to calculate the shape of the free surface, and since this theory is valid for Froude numbers close to $F = 1$, we start by examining the $F = 0.9$ case.

In order to find the waveless solutions to the weakly nonlinear problem, we start with a fixed Froude number F, low obstruction height ε and the obstruction separation b that results in waveless solutions in the nonlinear case. We then slowly increase or decrease this separation b until we find the point at which the waves change phase. An example of this phase change is included in Figure 2, where we observe five free surface profiles for fixed Froude number F and obstruction height ε with increasing separation b. We can then increase the obstruction height, using the waveless separation value from the previous height as our new starting guess. Repeating this process we can track the waveless contours in parameter space and plot these alongside the linear and nonlinear contours. As the KdV equation is valid for Froude numbers close to $F = 1$, we start by

https://doi.org/10.1017/S0956792516000449 Published online by Cambridge University Press

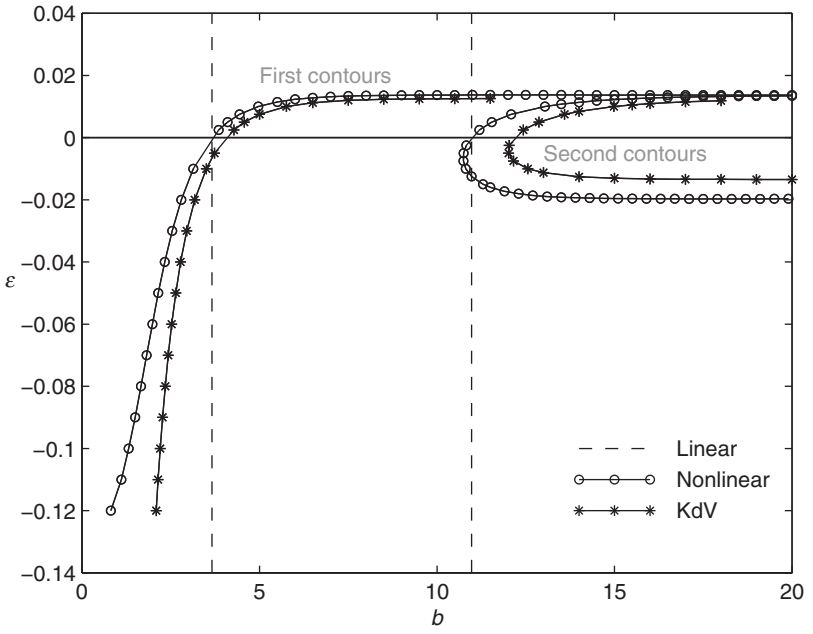

FIGURE 3. Contour plot showing the values of obstruction height ε and separation b that result in waveless solutions for $F = 0.9$.

comparing the contours for the $F = 0.9$ case, before comparing the contours for lower Froude numbers.

In Figure 3, we have contours in parameter space showing the obstruction height and separation values at which waveless solutions exist for a Froude number of $F = 0.9$. The first two contours for the linear, weakly nonlinear and fully nonlinear solutions are included for obstructions of both positive and negative heights. The linear solutions are obtained using a method based on that of Lamb [13], which is given in detail by Holmes *et al.* [12]. The linearised problem produces waveless solutions when the separation between the obstructions is $b = \frac{(2k+1)\pi}{\kappa}$, $k = 0, 1, 2, \ldots$, where κ is the positive real root of the transcendental equation $\frac{\tanh \kappa}{\kappa} = F^2$. The vertical dashed lines represent the solutions to the linearised problem and are independent of the obstruction height. Each of the circles represents a solution to the full nonlinear problem and each of the stars represents a waveless solution to the KdV equation. At this high Froude number, the nonlinear effects are very strong and the nonlinear contours quickly deviate from the linear values. We observe that the first of the positive contours curves away from $b = 0$, before following a continuous horizontal path at the maximum height. The second positive contour also curls away from $b = 0$ and follows the horizontal path of the first contour, almost joining up. The first negative contour continues from the first positive contour, but does not deviate from the linear values as quickly and has a fairly straight section in the middle with a slight curve towards $b = 0$ just before terminating. The second negative contour continues from the second positive contour, but turns abruptly and follows a horizontal path. This contour behaviour is quite different to the lower Froude number cases examined by Holmes *et al.* [12].

https://doi.org/10.1017/S0956792516000449 Published online by Cambridge University Press

The KdV contours follow the same general shape as the nonlinear contours, but are slightly offset. We also observe that the KdV curves do not approach the linear values as the obstruction height approaches zero, as the nonlinear curves do. The KdV contours for obstructions of positive height do, however, provide good agreement with the nonlinear contours as they level off, suggesting that the KdV equation would give a good approximation to this maximum height for waveless solutions at this value of Froude number.

The solutions for the free surface on the first of the positive contours have a dip above the obstruction that increases in depth as the obstruction increases in height. The solutions on the remaining contours have two dips, one above each obstruction, with a number of trapped waves in between. The solutions on the second positive contour have one half wave trapped between the obstructions, those on the third contour have one and a half trapped waves, those on the fourth have two and a half trapped waves and so on. This behaviour is consistent with the results of Holmes *et al.* [12].

Some interesting behaviour was observed, however, where the contours almost link up. The solutions on the first contour have a single trough above a single obstruction, but as the contour becomes horizontal and the obstructions separate, this trough in the free surface becomes broad and flat. The solutions from the second contour have one half wave trapped between two troughs, and as this contour becomes horizontal these solutions also widen, so that two wide troughs are observed with a broad half wave trapped in between. These solutions occur at almost the same obstruction height, with the height values differing only at the fourth decimal place at a separation of $b = 17$. Some of the solutions from each contour are included in Figure 4 for the same range of separation values. The solutions shown in Figure 4(a) are from the horizontal section of the first positive contour and those in Figure 4(b) are from the horizontal section of the second positive contour.

A comparison of weakly nonlinear and fully nonlinear waveless solutions is included in Figure 5. Each solution is taken from the respective contour for Froude number $F = 0.9$ and obstruction height $\varepsilon = 0.01$. In Figure 5(a), we compare solutions from the first contour, with the weakly nonlinear waveless solution occurring at an obstruction separation of $b = 5.755$ and the fully nonlinear solution occurring at a separation of $b = 4.9626$. Solutions from the second contour are compared in Figure 5(b), where the weakly nonlinear waveless solution corresponds to an obstruction separation of $b = 15$ and the fully nonlinear solution corresponds to a separation of $b = 13.042$. In each case the weakly nonlinear solution is of a similar shape to the fully nonlinear solution, with wider and deeper troughs. This can be partly attributed to the difference in separation values between the weakly nonlinear and fully nonlinear cases.

A comparison of the first two waveless contours for the $F = 0.8$ case is included in Figure 6. The contours for the $F = 0.8$ case are of a similar general shape to those for the $F = 0.9$ case, with the exception of the second negative contour, which continues downwards from the corresponding positive contour rather than abruptly turning and becoming horizontal. It is possible that the negative contours for the $F = 0.8$ case may exhibit some of the 'zig-zag' pattern behaviour shown by Holmes *et al.* [12] that occurs at lower Froude numbers, but this has not been fully investigated.

The $F = 0.6$ case is included in Figure 7. This case was examined in detail by Holmes *et al.* [12], who produced the first five contours for positive and negative obstruction

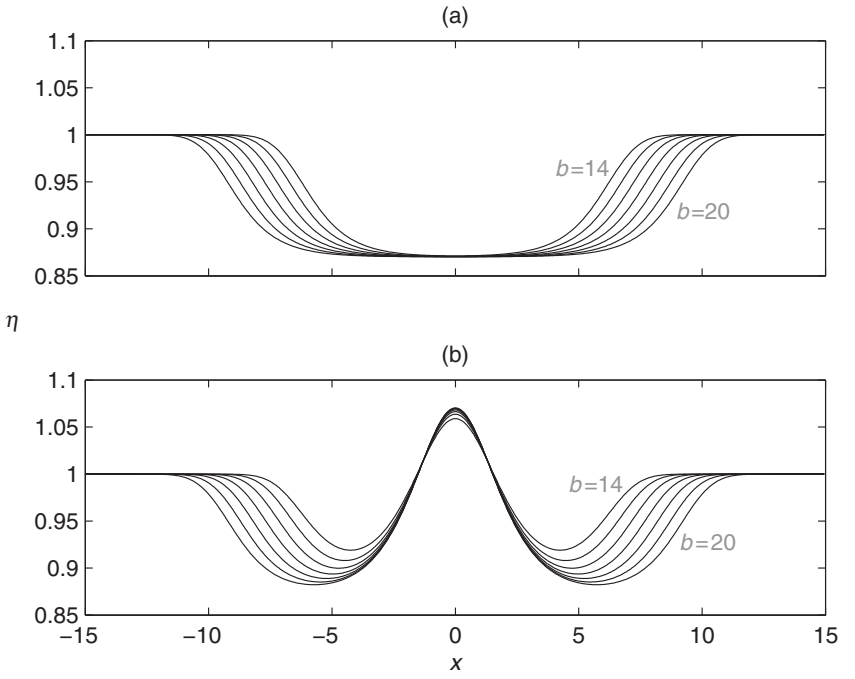

FIGURE 4. Nonlinear solutions from the horizontal sections of the positive contours from Figure 3. The solutions shown are for a Froude number of $F = 0.9$, with separation values $b = 14$, 15, 16, 17, 18, 19 and 20. (a) Solutions from the first contour, with obstruction height $\varepsilon = 0.0137$ and (b) solutions from the second contour, with obstruction heights increasing from $\varepsilon = 0.0114$ to $\varepsilon = 0.0135$.

heights as well as looped contours that originated from the ε-axis, but here we include only the first two contours and the upper looped contour in order to make a clearer comparison.

We observe that for these lower Froude numbers, $F = 0.8$ and 0.6, the KdV equation does not provide a good agreement with the nonlinear results and does not agree with the linear results in the limit as the obstruction height approaches zero. In the $F = 0.6$ case as shown in Figure 7, we note that the second KdV contour crosses the axis where the third linear and nonlinear curves would be (though not included). We also note that the nonlinear contours exhibit changing behaviour over the three cases, $F = 0.9$, 0.8 and 0.6, but the KdV contours all exhibit the same qualitative behaviour as the $F = 0.9$ case and do not follow the shape of the nonlinear contours for lower F values. These results are as expected, as the linear approximation is valid in the limit as the obstruction height ε tends to zero and the KdV approximation is valid in the limit as the Froude number F tends to one.

5.2 The effect of obstruction width

When solving the forced KdV equation for flow over a small bump with a narrow base, it is common to approximate the bump with a delta function, see, for example, Binder

https://doi.org/10.1017/S0956792516000449 Published online by Cambridge University Press

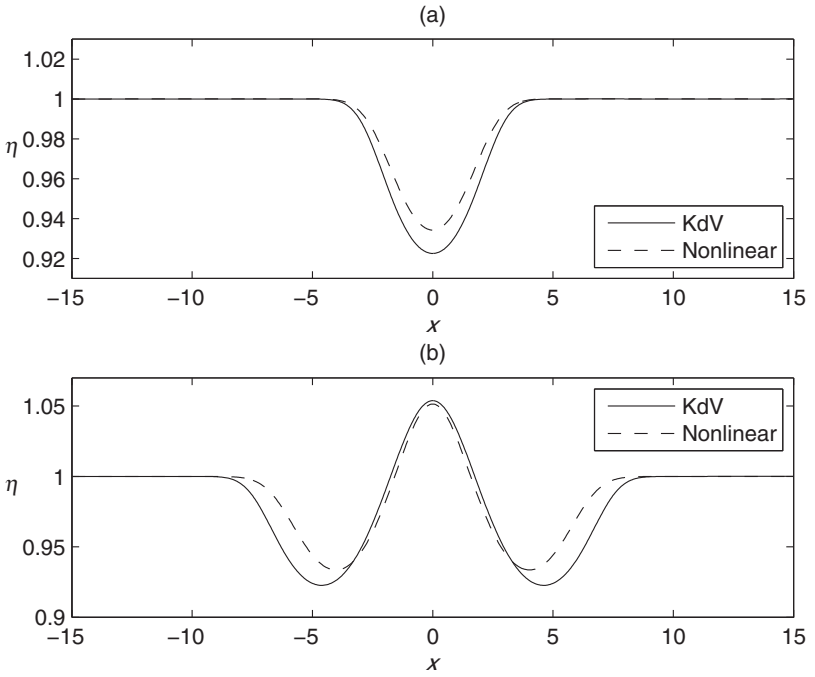

FIGURE 5. A comparison of weakly nonlinear and fully nonlinear waveless solutions for $F = 0.9$ and $\varepsilon = 0.01$. (a) Solutions from the first contour, with the weakly nonlinear solution occurring at the separation $b = 5.755$ and the fully nonlinear solution occurring at $b = 4.9626$. (b) Solutions from the second contour, where the weakly nonlinear solution occurs at the separation $b = 15$ and the fully nonlinear solution occurs at $b = 13.042$.

et al. [1, 2], Dias and Vanden-Broeck [5, 7] and Shen [16]. The area of the bump is used in the approximation, with the shape essentially neglected. We briefly examine part of the theory behind this method by looking at the effect of the obstruction width on the waveless solutions for our current problem, and compare results for obstructions of the same area but different widths and heights.

In Figure 8(a), we have contours that show the obstruction height and separation that result in waveless solutions for different width obstructions at a Froude number of $F = 0.9$. The contours in Figure 8(b) show the obstruction area and separation that result in the same waveless solutions. In each of these contour plots, four different width obstructions are considered, with the 'standard width' obstruction having a width coefficient of $w = 1$. We then have 'half width' obstructions with $w = 2$, 'quarter width' obstructions with $w = 4$ and 'double width' obstructions with $w = 0.5$. In the figure, solutions obtained using the numerical method for the fully nonlinear problem are represented by the shapes and the solutions obtained using the KdV equation are represented by the lines. We observe that obstructions of the same height with different widths produce quite different solutions, with a narrower obstruction capable of producing a waveless solution at a larger height. We also observe that obstructions of the same area with different widths produce more similar solutions, with the waveless contours appearing to approach some asymptotic limit

https://doi.org/10.1017/S0956792516000449 Published online by Cambridge University Press

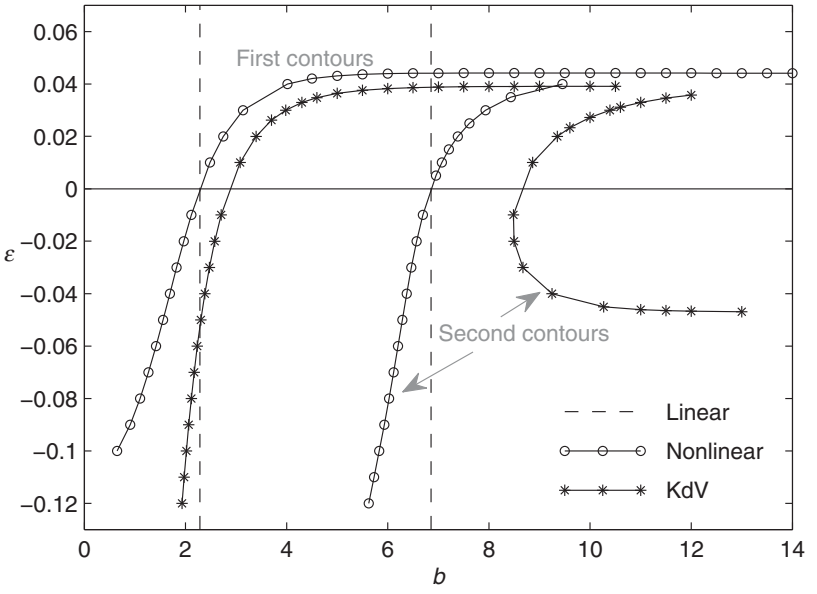

FIGURE 6. Contour plot showing the values of obstruction height ε and separation b that result in waveless solutions for $F = 0.8$.

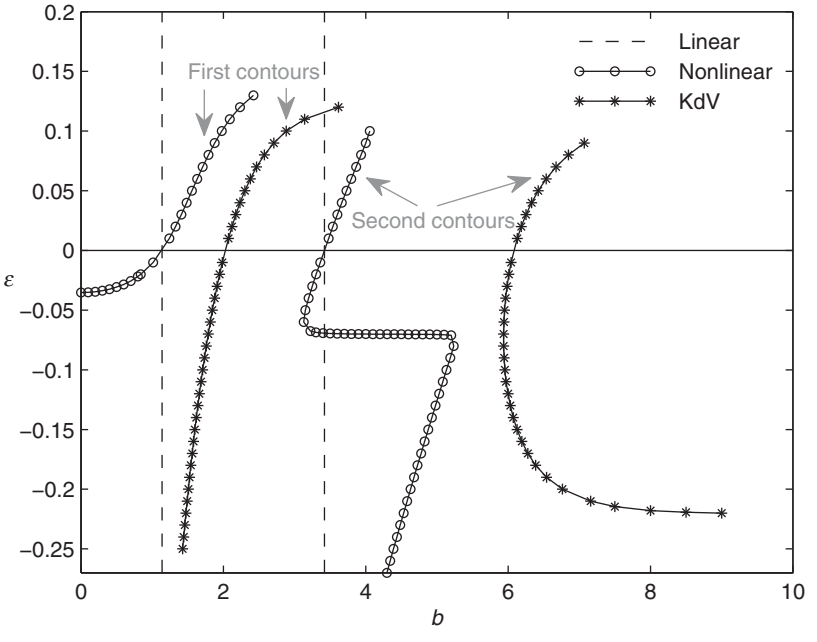

FIGURE 7. Contour plot showing the values of obstruction height ε and separation b that result in waveless solutions for $F = 0.6$.

https://doi.org/10.1017/S0956792516000449 Published online by Cambridge University Press

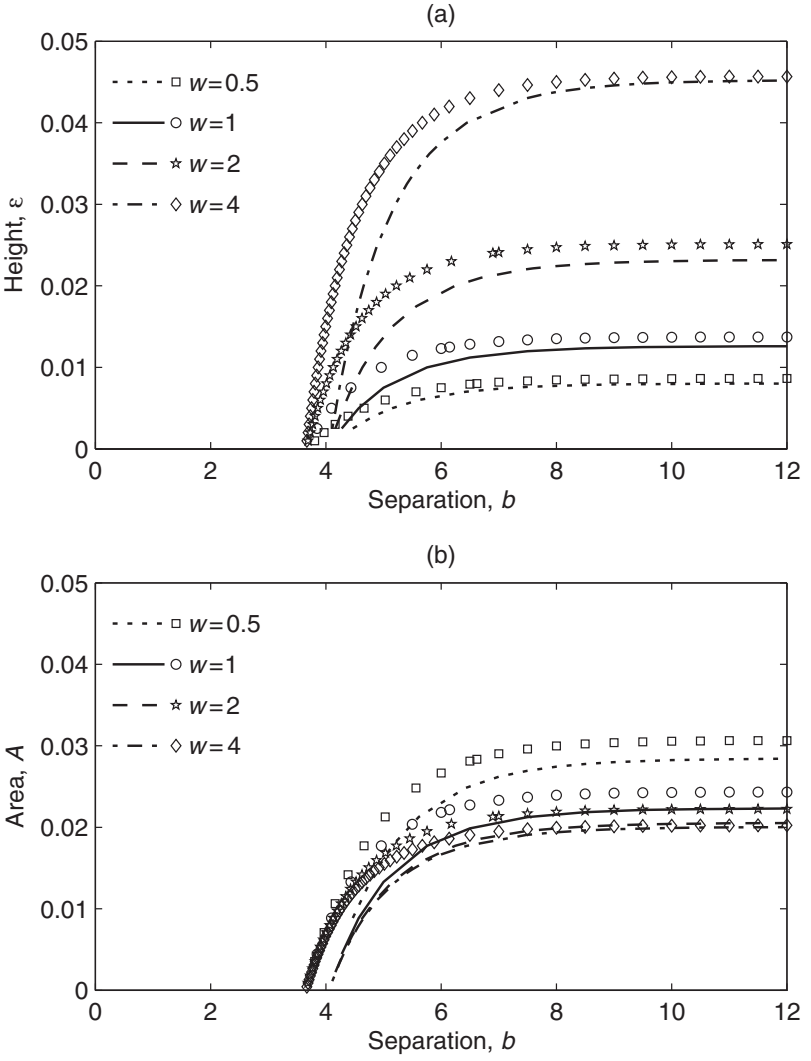

FIGURE 8. Contour plots showing the parameters that result in waveless solutions for different width obstructions for $F = 0.9$. The shapes indicate solutions to the nonlinear problem and the lines represent solutions to the KdV equation. We note that a larger w value represents a narrower obstruction.

as the obstruction width decreases. The KdV equation also appears to provide a more accurate comparison with the nonlinear solutions for narrower obstructions.

These results support the idea that for obstructions of small area and narrow base, the shape of the obstruction does not affect the parameters required for waveless solutions.

6 Conclusion

We have calculated waveless subcritical solutions for flow over Gaussian obstructions of both positive and negative heights, as an extension to the work of Forbes [8] and Holmes

https://doi.org/10.1017/S0956792516000449 Published online by Cambridge University Press

et al. [12]. The fully nonlinear and weakly nonlinear problems were solved numerically, and contours were plotted showing the values of obstruction height and separation at which waveless solutions exist. The contours for obstructions of positive height did not have any pairs that merged to form loops as was the case for the semi-ellipse considered by Forbes [8] and Hocking *et al.* [11]; however, in the higher Froude number cases, the positive contours followed a similar horizontal path through parameter space, almost linking up. Different free surface shapes were observed on each branch, suggesting the possibility of non-unique solutions.

Our interest in this problem of flow over topography is to find the parameter values that result in waveless solutions for a range of Froude numbers. The KdV equation does not offer the required level of accuracy in these parameters for Froude numbers lower than $F \simeq 0.9$. However, it does provide some qualitative properties of the wave behaviour.

The effect of width was also examined, with results suggesting that small, narrow obstructions of different height and width but the same area would produce similar solutions, as expected. Also, as the obstructions become narrower, the area approximation becomes more accurate.

Future work would involve developing a method to use the forced KdV equation to automatically find the parameters that result in waveless solutions. We would use it to calculate the waveless contours and analyse solution behaviour for Froude numbers close to $F = 1$. This way we could extend the contours for the $F = 0.9$ case and closely examine the apparent linking of contours without the restriction of the long computation times that come with the numerical method for the fully nonlinear problem.

References

[1] Binder, B. J., Dias, F. & Vanden-Broeck, J.-M. (2005) Forced solitary waves and fronts past submerged obstacles. *Chaos* **15**, 037106-1–037106-13.

[2] Binder, B. J., Dias, F. & Vanden-Broeck, J.-M. (2008) Influence of rapid changes on free surface flows. *IMA J. Appl. Math.* **73**, 254–273.

[3] Choi, J. W., An, D., Lim, C. & Park, S. (2003) Symmetric surface waves over a bump. *J. Korean Math. Soc.* **40**, 1051–1060.

[4] Dias, F. & Vanden-Broeck, J.-M. (1989) Open channel flows with submerged obstructions. *J. Fluid Mech.* **206**, 155–170.

[5] Dias, F. & Vanden-Broeck, J.-M. (2002) Generalised critical free surface flows. *J. Eng. Math.* **42**, 291–301.

[6] Dias, F. & Vanden-Broeck, J.-M. (2002) Steady two-layer flows over an obstacle. *Phil. Trans. R. Soc. Lond. A* **360**, 2137–2154.

[7] Dias, F. & Vanden-Broeck, J.-M. (2004) Trapped waves between submerged obstacles. *J. Fluid Mech.* **509**, 93–102.

[8] Forbes, L. K. (1982) Non-linear, drag-free flow over a submerged semi-elliptical body. *J. Eng. Math.* **16**, 171–180.

[9] Forbes, L. K. (1988) Critical free-surface flow over a semi-circular obstruction. *J. Eng. Math.* **22**, 3–13.

[10] Forbes, L. K. & Hocking, G. C. (2007) An intrusion layer in stationary incompressible fluids: Part 2: A solitary wave. *Eur. J. Appl. Math.* **17**, 577–595.

[11] Hocking, G. C., Holmes, R. J. & Forbes, L. K. (2013) A note on waveless subcritical flow past a submerged semi-ellipse. *J. Eng. Math.* **81** 1–8.

https://doi.org/10.1017/S0956792516000449 Published online by Cambridge University Press

[12] Holmes, R. J., Hocking, G.C., Forbes, L. K. & Baillard, N. Y. (2013) Waveless subcritical flow past symmetric bottom topography. *Eur. J. Appl. Math.* **24**, 213–230.
[13] Lamb, H. (1932) *Hydrodynamics*, 6th ed., Cambridge University Press, Cambridge.
[14] Lustri, C. J., McCue, S. W. & Binder, B. J. (2012) Free surface flow past topography: a beyond-all-orders approach. *Eur. J. Appl. Math.* **23**, 441–467.
[15] Pratt, L. J. (1984) On nonlinear flow with multiple obstructions. *J. Atmos. Sci.* **41**, 1214–1225.
[16] Shen, S. S.-P. (1995) On the accuracy of the stationary forced Korteweg-de Vries equation as a model equation for flows over a bump. *Q. Appl. Math.* **53**, 701–719.
[17] Sivakumaran, N. S., Tingsanchali, T. & Hosking, R. J. (1983) Steady shallow flow over curved beds. *J. Fluid Mech.* **128**, 469–487.